ISBN: 978-3-95450-206-6 doi:10.18429/JACoW-FLS2018-TUA2WC01

TRANSPORTATION AND MANIPULATION OF A LASER PLASMA ACCELERATION BEAM*

A. Ghaith†, T. André, A. Loulergue, M. Labat, D. Oumbarek, C. Kitegi, I. Andriyash, F. Briquez, M. Valléau, F. Marteau, O. Marcouillé, F. Blache, F. Bouvet, Y. Dietrich, J. P. Duval, M. El-Ajjouri, C. Herbeaux, N. Hubert, N. Leclercq, A. Lestrade, P. Rommeluere, M. Sebdaoui, K. Tavakoli, M. E. Couprie, Synchrotron SOLEIL, GIF-sur-YVETTE , France
C. Thaury, G. Lambert, S. Corde, J. Gautier, B. Mahieu, K. Ta Phuoc, V. Malka, Laboratoire d'Optique Appliquée, Orsay, France
E. Roussel, Bielawski, C. Evain, C. Szwaj, Laboratoire PhLAM, Lille, France

Abstract

The ERC Advanced Grant COXINEL aims at demonstrating free electron laser amplification, at a resonant wavelength of 200 nm, based on a laser plasma acceleration source. To achieve the amplification, a 8 m long dedicated transport line was designed to manipulate the beam qualities. It starts with a triplet of permanent magnet with tunable gradient quadrupoles (QUAPEVA) that handles the highly divergent electron beam, a demixing chicane with a slit to reduce the energy spread per slice, and a set of electromagnetic quadrupoles to provide a chromatic focusing in a 2 m long cryogenic undulator. Electrons of energy 176 MeV were successfully transported throughout the line, where the beam positioning and dispersion were controlled efficiently thanks to a specific beam based alignment method, as well as the energy range by varying the slit width. Observations of undulator radiation for different undulator gaps are reported.

INTRODUCTION

Laser Plasma Acceleration (LPA) [1–3] has proven to be an efficient way to produce high energy electrons within a short accelerating distance. It can produce a GeV electron beam within a distance of few cms [4], high peak current up to 10 kA and short bunch length (few fs). However, the divergence is quite high of the order of few mrads and so is the energy spread (few %) [5]. A powerful laser focused on a gas chamber ionizes the gas molecules and pushes the electrons out of its path leaving the ions un-affected. This induces a plasma wave with an intense electric field following the direction of the laser. The electron beam caught in between the laser pulse and the plasma wave is accelerated until it surpasses the wave and thus attains maximum energy possible.

Undulator radiation has been successively observed [6–10] using LPA source, while Free Electron Laser (FEL) based applications remain very challenging due to the beam quality that does not fit the FEL requirements:

$$\begin{cases} \epsilon_N < \frac{\gamma\lambda}{4\pi} \\ \sigma_\gamma < \rho \end{cases} \quad (1)$$

where ϵ_N is the normalized emittance, γ the Lorentz factor, λ the radiation wavelength to be amplified, σ_γ the energy spread (FWHM) and ρ the pierce parameter:

$$\rho = \left[\frac{1}{16}\frac{I_{peak}}{I_A}\frac{\lambda_u^2 K^2 [JJ]^2}{4\pi^2\gamma^2\sigma_x\sigma_z}\right]^{1/3} \quad (2)$$

where I_{peak} is the peak current, I_A the Alfven current (17 kA), λ_u the undulator magnetic period, K the deflection parameter proportional to the undulator peak field and period, $[JJ] = J_0(\kappa) - J_1(\kappa)$ ($\kappa = \frac{K^2}{4+2K^2}$), σ_x and σ_z are the horizontal and vertical beam size (rms) respectively.

COXINEL [11–19], among other LPA based projects [20, 21], aims at demonstrating FEL amplification by the help of a dedicated transport line to handle and manipulate the beam properties [22].

BEAM MANIPULATION LINE

The line starts by focusing an intense Sa:Ti laser (800 nm) with 30 TW power, 1.5 mJ energy and 30 fs pulse duration on a gas jet composed of 99% He and 1% N_2. The baseline reference case of the slice beam parameters produced are shown in Table 1 (source). High gradient quadrupoles (~200 T/m) are used to decrease the beam divergence, and a chicane accompanied with a slit to select the desired energy. Table 1 (undulator) presents the electron beam parameters after beam manipulation. The divergence is reduced by a factor of 10 with a beam size of 50 μm corresponding to a normalized emittance of 1.7 mm.mrad that satisfy the first FEL condition. The slice energy spread is reduced by a factor of 10 on the expense of the peak current where the beam is decompressed (longer bunch length). Thus FEL amplification is feasible after such manipulation.

* Work supported by SOLEIL
† amin.ghaith@synchrotron-soleil.fr

ISBN: 978-3-95450-206-6 doi:10.18429/JACoW-FLS2018-TUA2WC01

Table 1: COXINEL Baseline Reference Case at the Source and at the Undulator after Beam Manipulation

Slice Parameters	Source	Undulator
Divergence	1 mrad	0.1 mrad
Beam size	1 μm	50 μm
Bunch length (rms)	3.3 fs	33 fs
Charge	34 pC	34 pC
Peak Current	4.4 kA	440 A
σ_γ	1% rms	0.1% rms
ϵ_N	1 mm.mrad	1.7 mm.mrad

MAGNETIC ELEMENTS

The first magnetic element placed 5 cm after the gas jet is a triplet of permanent magnet based quadrupoles with high tunable gradient (QUAPEVAs) [23]; followed by a chicane composed of four electro-magnet dipoles; a set of four electro-magnet quadrupoles to ensure good focusing inside the undulator; a cryo-ready undulator and finally a dipole dump (see Fig. 1).

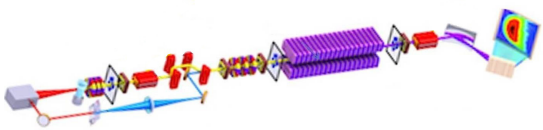

Figure 1: Schematic view of COXINEL transport line. Left to right: Laser, gas jet, permanent magnet quadrupoles [23], four electro-magnet dipoles (chicane), four electro-magnet quadrupoles, undulator and dipole dump.

QUAPEVAs

The QUAPEVA [23] is composed of two superimposed quadrupoles, one placed at the center following a Halbach configuration, surrounded by another that consists of four rotating cylindrical magnets to provide the gradient variability (see Fig.2). Table 2 shows the QUAPEVA parameters alongside the characteristics of the magnets and poles.

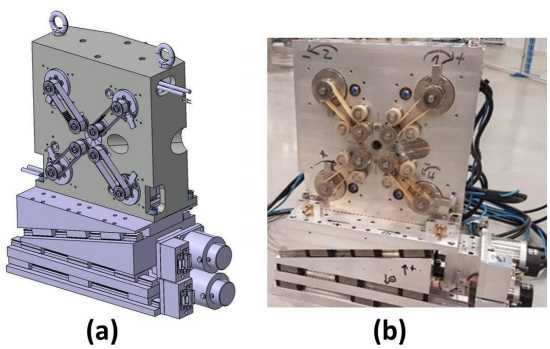

Figure 2: (a) mechanical design, (b) actual device.

Table 2: QUAPEVA Parameters

Parameters	Value	Unit
Gradient (G)	110 - 200	T/m
Remanent Field (B_r)	1.26	T
Coercivity (H_{cj})	1830	kA/m
Pole saturation	2.35	T

Chicane

The chicane consists of four electro-magnet dipoles with a maximum field of 0.55 T. Figure 3 shows the dipoles installed on the transport line. In the center, an adjustable slit with varying width is placed [24, 25]. Once the beam passes through the first two dipoles it is dispersed longitudinally and horizontally as shown in Fig. 4, and by closing the slit one is able to select a smaller energy range.

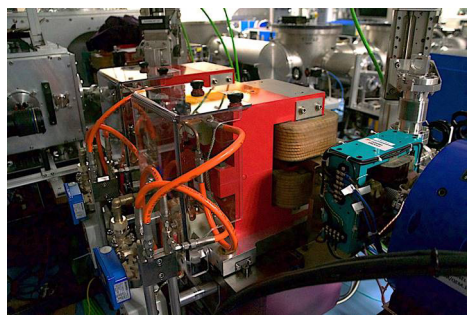

Figure 3: Second section of the chicane.

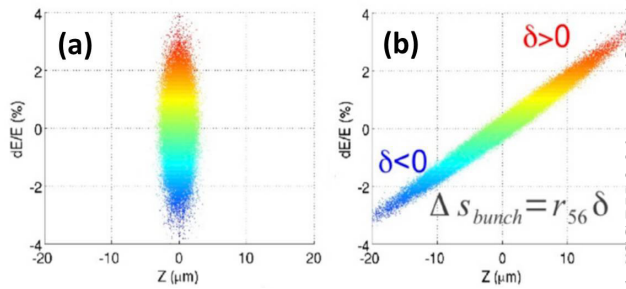

Figure 4: (a) Electron beam before the chicane, (b) after the first two dipoles of the chicane.

Quadrupoles

A set of four electro-magnet quadrupoles is installed after the chicane as shown in Fig. 5 to enable good focusing inside the undulator. The magnetic length of the quadrupole is 200 mm with a maximum gradient attained at 20 T/m.

ISBN: 978-3-95450-206-6 doi:10.18429/JACoW-FLS2018-TUA2WC01

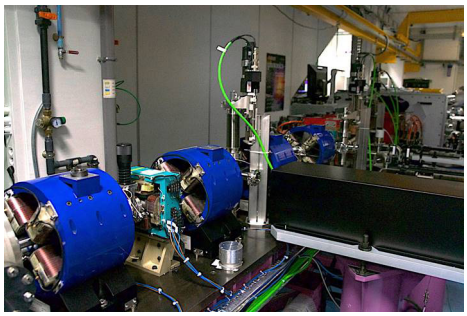

Figure 5: Set of four electro-magnet quadrupoles (blue) and a steerer (cyan) in between the last two.

ELECTRON BEAM DIAGNOSTICS

Electron beam diagnostics are installed all along the line [26]. Five scintillator screens (YAG and LANEX) placed: after the first set of quadrupoles, inside the chicane, before undulator, after undulator and after dipole dump. Two Integrated Current Transformers (ICTs) to measure the beam charge: one after the first set of quadrupoles and one after the undulator.

Beam Transport

The energy of the beam produced ranges from 50 MeV to 200 MeV. Figure 6 shows an electron beam measurement using a dipole and an electron spectrometer placed after the gas jet. The vertical divergence per slice (±5 MeV) is around 1.5 mrad rms.

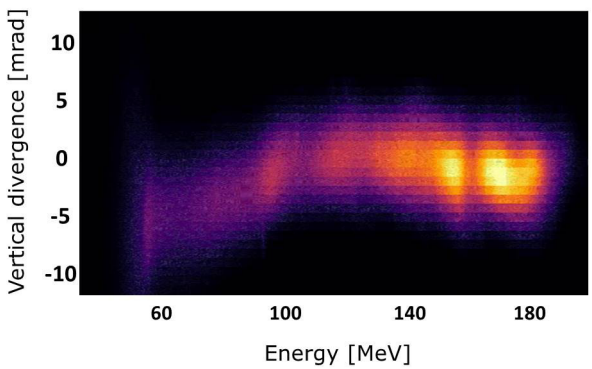

Figure 6: Electron beam measured using a dipole and an electron spectrometer.

Figure 7 shows an electron beam measurement at screen 1 (after the QUAPEVAs) without (a) and with the triplet (b). The large divergent beam is well focused, where the horizontal size is reduced by a factor of 3 and the vertical size by a factor of 2. The cross shape is due to the large energy spread that leads to chromatic effects. Figure 8 shows the electron beam measured at different locations of the transport line (Top) compared to the simulation (Bottom), and they show a very good agreement. The electron beam measured is tilted compared to the simulations due to the skew quadrupolar term of the QUAPEVAs, it has been later corrected using mechanical shims.

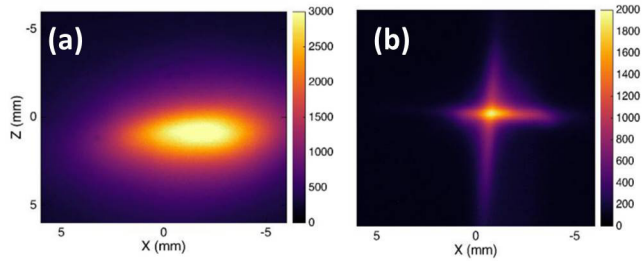

Figure 7: Measured electron beam on a Lanex screen placed 64 cm away from the first set of quadrupoles. (a) without QUAPEVAs, (b) with QUAPEVAs.

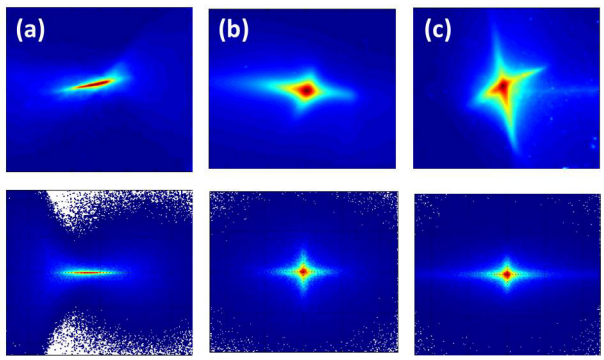

Figure 8: Electron beam measured (Top) and computed (Bottom) along the line. (a): Imager 2 (middle of chicane), (b): Imager 4 (before the undulator), (c) Imager 5 (after the undulator.

PHOTON SOURCE

The source of radiation is a cryo-ready undulator (parameters shown in Table 3), meaning it can function at both room and cryogenic temperatures [27–30]. It is currently operating at room temperature due to infrastructure reasons. Figure 9 shows the undulator installed at COXINEL, it consists of a carriage with a metallic base where the girders are separated by a gap and can be varied by two steps motors.

Table 3: Undulator Parameters

Parameters	Value
Technology	Hybrid cryogenic
Magnet material	CR53-Hitachi ($Pr_2Fe_{14}B$)
Remanence field	1.32 T
Coercivity	1.63 T
Pole material	Vanadium Permendur
Period	18 mm
No of periods	107

ISBN: 978-3-95450-206-6 doi:10.18429/JACoW-FLS2018-TUA2WC01

The resonant wavelength emitted (λ) is expressed as follows:

$$\lambda = \frac{\lambda_u}{2\gamma^2}\left[1 + \frac{K^2}{2} + \gamma^2\theta^2\right] \quad (3)$$

where λ_u is the undulator period, γ the Lorentz factor, $K = 93.4B[\mathrm{T}]\lambda_u[\mathrm{m}]$ the deflection parameter, B the peak field and θ the angle of the emitted radiation with respect to the observer.

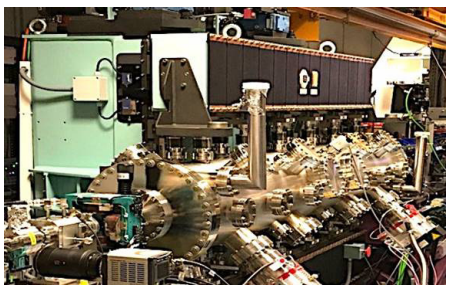

Figure 9: Undulator picture installed on COXINEL transport line.

The undulator can be closed to a minimum gap value of 4.55 mm and vary up to 30 mm. The magnetic field computed by RADIA [31] and measured with a Hall probe versus gap are shown in Fig. 10-a. For an energy of 176 MeV, the radiation spans between 180 nm - 280 nm (see Fig. 10-b).

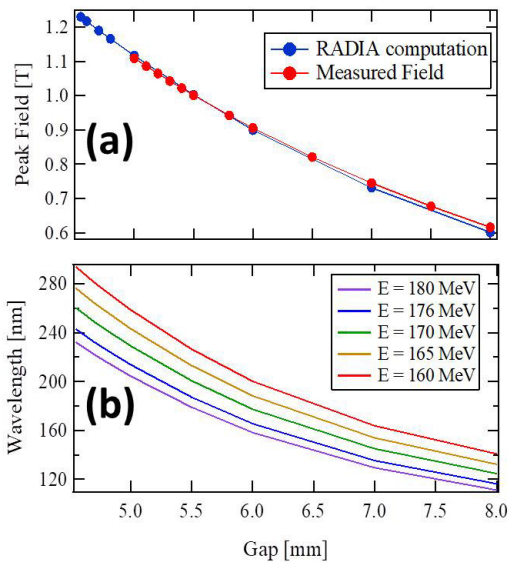

Figure 10: (a) peak field computed (blue) and measured (red) versus undulator gap. (b) theoretical wavelength calculated using Eq. 3.

PHOTON BEAM DIAGNOSTICS

Angular Flux

A Charge Couple Device (CCD) camera is installed 3 m from the exit of the undulator as shown in Fig. 11. Three optical filters were tested: centered around 200 nm with 10 nm bandwidth, centered at 254 nm with 38 nm bandwith; centered at 300 nm with 45 nm bandwidth.

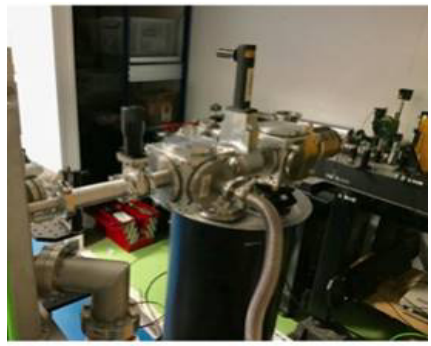

Figure 11: CCD camera installed 3 m from the exit of the undulator.

Figure12a presents a computation of the transverse photon beam shape using SRWE [32] with electron beam parameters computed by beta code. Fig 12-b shows the integrated instensity measurements with the CCD camera compared to simulations for four different optical filter cases (No filter, 300 nm, 254 nm and 200 nm filter). In the case where no optical filter is applied (black), the window captures all the radiation emitted which scales as an exponential decay versus gap ($P \propto B^2$) and the intensity drops when the optical filters are applied. For small gaps (5 mm - 6 mm) there is a bump for the 200 nm filter case, and that is caused by the fact that the on-axis radiation (resonance) have a spectral flux ~ half of the off-axis ones.

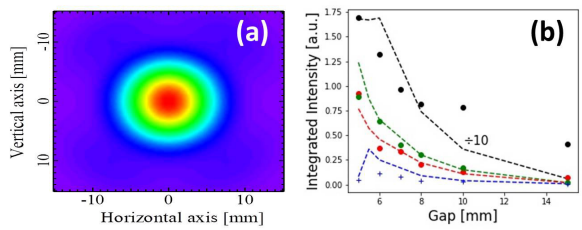

Figure 12: (a) Transverse beam shape computed. (b) Integrated intensity measured by the CCD camera (points) and computed using SRWE (dashed). Different optical filters applied: (red) centered at 300 nm with a 45 nm bandwidth, (green) centered at 254 nm optical filter with a 38 nm bandwidth, (blue) centerd at 200 nm with 10 nm bandwidth, (black) no filter is applied.

Spectral Flux

An iris is placed 2.28 m from the last magnet of the undulator, immediately followed by a spherical lens of focal length 240 mm to focus the radiation at the spectrometer slit placed at a distance equal to the focal length (see Fig. 13).

The flux has been measured with the spectrometer for different undulator gaps. Figure14 shows one of these measurements for a 4.55 mm gap.

ISBN: 978-3-95450-206-6 doi:10.18429/JACoW-FLS2018-TUA2WC01

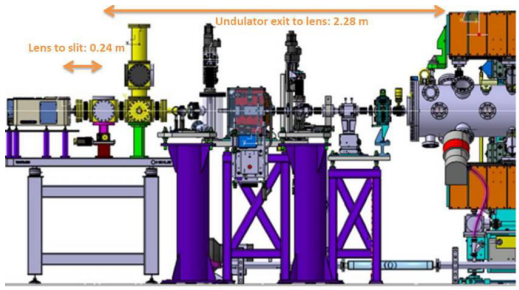

Figure 13: schematic view of photon beam diagnostic line. left to right: undulator, steerer, dipole dump, lens, spectrometer.

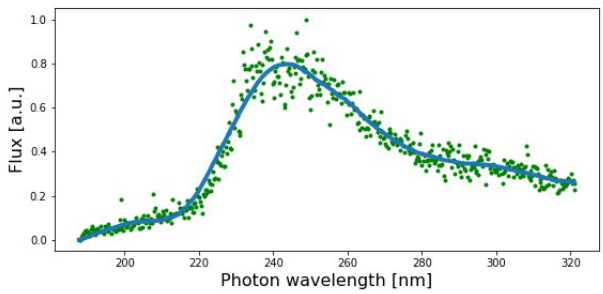

Figure 14: Spectral flux measured with the spectrometer.

CONCLUSION

The COXINEL line enables to control, manipulate and transport of a highly divergent beam produced by laser plasma acceleration source. High gradient permanent magnet quadrupoles enable beam pointing alignment compensation (position control and dispersion compensation) thanks to the transverse adjustable tables. The chicane accompanied with a slit provides a reduction in the energy spread. Undulator radiation has been measured using a CCD camera (Transverse beam shape) and a spectrometer (spectral flux) for different undulator gaps, and gave insight on the electron beam parameters. By further improving the beam quality, attaining free electron laser amplification is not that far fetched.

ACKNOWLEDGEMENT

The authors are very grateful for the support of the European Research Council (ERC) for COXINEL (340015) and the "Triangle de la Physique" for the QUAPEVAs contract.

REFERENCES

[1] T. Tajima, and J. M. Dawson. "Laser electron accelerator." *Physical Review Letters* 43.4 (1979): 267.

[2] E. Esarey, C. Schroeder, and W. Leemans, Physics of laser-driven plasma-based electron accelerators, *Reviews of Modern Physics*, vol. 81, no. 3, pp. 1229, 2009.

[3] V. Malka, J. Faure, C. Rechatin, A. Ben-Ismail, J. Lim, X. Davoine, and E. Lefebvre, Laser-driven accelerators by colliding pulses injection: A review of simulation and experimental results, *Physics of Plasmas(1994-present)*, vol. 16, no. 5, pp. 056703, 2009.

[4] W P. Leemans, *et al.* "Multi-GeV electron beams from capillary-discharge-guided subpetaWatt laser pulses in the self-trapping regime," *Physical Review Letters*, vol. 113, p. 245002, Dec 2014.

[5] C. Rechatin,J. Faure, A. Ben-Ismail, J. Lim, R. Fitour, A. Specka, H. Videau, A. Tafzi, F. Burgy, V. Malka, "Controlling the Phase-Space Volume of Injected Electrons in a Laser-Plasma Accelerator", *Physical Review Letters*, vol. 102, no. 16, pp. 164801, 2009.

[6] H.-P. Schlenvoigt, K. Haupt, A. Debus, F. Budde, O. Jäckel, S. Pfotenhauer, H. Schwoerer, E. Rohwer, J. Gallacher, E. Brunetti, R. Shanks, S. Wiggins, and D. Jaroszynski, "A compact synchrotron radiation source driven by a laser-plasma wakefield accelerator," *Nature Physics*, vol. 4, no. 2, pp. 130–133, 2008.

[7] M. Fuchs, R. Weingartner, A. Popp, Z. Major, S. Becker, J. Osterhoff, I. Cortrie, B. Zeitler, R. Hörlein, G. D. Tsakiris, U. Schramm, T. Rowlands-Rees, S. Hooker, D. Habs, F. Krausz, S. Karsch, and F. Grüner, "Laser-driven soft-X-ray undulator source," *Nature physics*, vol. 5, no. 11, pp. 826–829, 2009.

[8] M. P. Anania *et al.*, "The ALPHA-X beam line: toward a compact FEL," in *Proc. IPAC* 2010 , vol. 5, paper TUPE052, pp. 2263–2265.

[9] G. Lambert, S. Corde, K. T. Phuoc, V. Malka, A. B. Ismail, E. Benveniste, A. Specka, M. Labat, A. Loulergue, R. Bachelard, and M.-E. Couprie, "Progress on the generation of undulator radiation in the UV from a plasma-based electron beam," in *Proc. FEL conf., Nara, Japan* , paper THPD47, pp. 2, 2012.

[10] Plasma accelerator produces first X-rays, `http://www.desy.de/news/news_search/index_eng.html?openDirectAnchor=1261&two_columns=0`

[11] M.-E. Couprie *et al.*,"The LUNEX5 project in France",*Journal of Physics: Conference Series*, vol. 425, n0. 7,pp. 072001, 2013.

[12] M.-E. Couprie *et al.*, "Progress of the LUNEX5 project," in *35th International Free-Electron Laser Conference (FEL 2013)*, New York, NY, USA, Nov. 2013, paper WEPSO05, pp. 502–506.

[13] M.-E. Couprie *et al.*, "Strategies towards a compact XUV free electron laser adopted for the LUNEX5 project," *Journal of Modern Optics*, pp. 1–13, 2015.

[14] M.-E. Couprie *et al.*, "Experiment preparation towards a demonstration of laser plasma based free electron laser amplification", *Proc. FEL'14 (Basel, Switzerland*, paper TUP086, pp. 596.

[15] A. Loulergue, M. Labat, C. Evain, C. Benabderrahmane, V. Malka, and M. Couprie, "Beam manipulation for compact laser wakefield accelerator based free-electron lasers," *New Journal of Physics*, vol. 17, no. 2, pp. 023028, 2015.

[16] M.-E. Couprie *et al.*, "An application of laser–plasma acceleration: towards a free-electron laser amplification," *Plasma Physics and Controlled Fusion*, vol. 58, no. 3, pp. 034020, 2016.

[17] André Thomas *et al*., First electron beam measurements on COXINEL." 7th International Particle Accelerator Conference (IPAC'16), Busan, Korea. 2016.

ISBN: 978-3-95450-206-6 doi:10.18429/JACoW-FLS2018-TUA2WC01

[18] André, Thomas *et al.*, "Electron Transport on COXINEL Beam Line." 8th Int. Particle Accelerator Conf.(IPAC'17), Copenhagen, Denmark, 14â 19 May, 2017. JACOW, Geneva, Switzerland, 2017.

[19] M.-E. Couprie *et al.*, "Towards free electron laser amplification to qualify laser plasma acceleration", *The review of laser engineering*, 45(2):94–98, 2017.

[20] C. B. Schroeder *et al.*, "Application of Laser Plasma Accelerator beams to Free-Electron Laser," 2012 Proc. FEL, Nara, Japan, paper THPD57, pp. 658–61.

[21] M.P. Anania *et al.*, "An ultrashort pulse ultra-violet radiation undulator source driven by a laser plasma wakefield accelerator," *Applied Physics Letters*, vol. 104, no. 26, pp. 264102, 2014.

[22] Loulergue A *et al*., Beam manipulation for compact laser wakefield accelerator based free-electron lasers. New J. Phys. 17, 023028 (2015).

[23] F. Marteau, A. Ghaith, P. N'Gotta, C. Benabderrahmane, M. Valléau, C. Kitegi et al... Variable high gradient permanent magnet quadrupole (QUAPEVA). Applied Physics Letters, 111(25), 253503.

[24] A. Maier, A. Meseck, S. Reiche, C. Schroeder, T. Seggebrock, and F. Gruener, "Demonstration scheme for a laser-plasma-driven free-electron laser," *Physical Review X*, vol. 2, no. 3, pp. 031019, 2012.

[25] M.-E. Couprie, A. Loulergue, M. Labat, R. Lehe, and V. Malka, "Towards a free electron laser based on laser plasma accelerators," *Journal of Physics B: Atomic, Molecular and Optical Physics*, vol. 47, no. 23, pp. 234001, 2014.

[26] Labat, M., Hubert, N., El Ajjouri, M., Cassinari, L., Bourrassin-Bouchet, C., Loulergue, A., Couprie, M. E. (2014). Electron beam diagnostics for COXINEL. THP087, these proceedings, FEL, 14.

[27] Benabderrahmane, C., Valléau, M., Berteaud, P., Tavakoli, K., Marlats, J.L., Nagaoka, R., Béchu, N., Zerbib, D., Brunelle, P., Chapuis, L. and Dallé, D., 2013. Development of a 2 m Pr2Fe14B cryogenic permanent magnet undulator at SOLEIL. *In Journal of Physics: Conference Series* Vol. 425, No. 3, p. 032019 .

[28] Couprie, M.E., Briquez, F., Sharma, G., Benabderrahmane, C., Marteau, F., Marcouillé, O., Berteaud, P., El Ajjouri, T., Vétéran, J., Chapuis, L. and Valléau, M., 2015, May. Cryogenic undulators. "In Advances in X-ray Free-Electron Lasers Instrumentation III" *International Society for OpticsandPhotonics.* Vol. 9512, p. 951204

[29] Valléau, M., Benabderrahmane, C., Briquez, F., Berteaud, P., Tavakoli, K., Zerbib, D., Chapuis, L., Marteau, F., Marcouillé, O., El Ajjouri, T. and Vétéran, J., 2016, July. Development of cryogenic undulators with PrFeB magnets at SOLEIL. In AIP Conference Proceedings (Vol. 1741, No. 1, p. 020024). AIP Publishing.

[30] Benabderrahmane, C., Valléau, M., Ghaith, A., Berteaud, P., Chapuis, L., Marteau, F., ... Mary, A. (2017). Development and operation of a $Pr_2Fe_{14}B$ based cryogenic permanent magnet undulator for a high spatial resolution x-ray beam line. *Physical Review Accelerators and Beams*, 20(3), 033201 .

[31] Chubar, Oleg, Pascal Elleaume, and Joel Chavanne. "A three-dimensional magnetostatics computer code for insertion devices." Journal of synchrotron radiation 5.3 (1998): 481-484.

[32] Chubar, Oleg, and P. Elleaume. "Accurate and efficient computation of synchrotron radiation in the near field region." proc. of the EPAC98 Conference. 1998.